Novel bioactive composites fabricated by freezing-thawing method for bone regeneration applications.

+Maria Canillas [1], +Gabriel G. de Lima [2], Miguel .A. Rodríguez [1], *Michael J.D. Nugent[2], Declan M. Devine [2,3]

[1] Ceramic and Glass Institute from CSIC, Madrid, Spain.

[2] Materials Research Institute, Athlone Institute of Technology, Athlone, Ireland

[3] Rehabilitation Medicine Centre, Mayo Clinic, Rochester, MN, USA.

+ Authors contributed equally to work

Declan M. Devine, email: ddevine@ait.ie

*Correspondence to: Michael J.D. Nugent. Tel: +353 9064 68172; fax: +353 0964 68148; e-mail address: mnugent@ait.ie

ABSTRACT

Hydrogels are widely used for controlled delivery of therapeutic agents. However, hydrogels lack bioactivity to encourage bone formation and required mechanically integrity. Moreover, chemically crosslinking hydrogels exhibits cytotoxic effect. To overcome these issues poly-vinyl alcohol (PVA) and poly-acrylic acid (PAA) blends were utilised as a polymer matrix and were combined with a ceramic materials consists of βTCP, Wollastonite and Magnesium silicate. The final 3D construct was physically crosslinked using various freeze thawing (F/T) cycles. The final composite were characterized by FTIR, SEM, swelling and rheometry. Antimicrobial activity containing ciprofloxacin was tested against a pathogen associated with osteomyelitis. FTIR and SEM analysis illustrated that ceramics were dispersed within the composite and improved the hydrogen bonds of these hydrogels which had a porous morphology. Swelling studies in buffer solution pH 7.4 showed an increase in polymer swelling when ceramic was added. However, rheological testing demonstrated that incorporation of ceramics caused an increase in mechanical properties. DSC thermograms showed increased T_g values for samples containing ceramics. Antimicrobial activity tests presented positive results with ciprofloxacin. The combination of increased strength and ability to encapsulate a clinically relevant antimicrobial agent indicates that the composite tested in this study has potential for the treatment of osteomyelitis.

INTRODUCTION

Bone is often thought be a solid inert material. However, the long bones of the arms and legs are in fact highly complex tissues which

undergo microfracture and repair through everyday loading. It is this ability to repair and regenerate its structure that enables bone to spontaneously repair itself following injury without the formation of scar tissue [1]. However in 5-10% of all fractures are associated with impaired healing, resulting from high-energy traumatic events, or surgical interventions to treat a variety of ailments including osteomyelitis [2]. The standard treatment for osteomyelitis is the surgical removal or debridement of infected tissue and the treatment of the resultant bone defect with a bone grafting procedure. These bone grafting procedures have well known complications such as donor site morbidity, limited supply and the risk of disease and infection transmission [3–5]. Moreover, if the pathogen is not completely removed during surgery, a reoccurrence of the osteomyelitis can occur [6]. Complications related to infection are the number one cause for orthopedic revision surgeries. In these instances there is an urgent need to develop a suitable synthetic alternative to bone grafting that actively treats or prevents reoccurrence of infections.

To meet the requirement of an ideal material, the bone substitute material ought to be: biocompatible, biodegradable, bioactive, osteoconductive, osteoinductive or a combination thereof [7]. Moreover, the structure should be porous to enable bone and blood vessel infiltration [8]. Numerous biodegradable, biocompatible and biostable polymers have been suggested and studied for this application including hydrogels [9]. Hydrogels have been used widely in biomaterial applications, mainly due to their low interfacial tension, useful swelling properties and high lubricity. In addition to their promising biocompatibility characteristics, certain hydrogels are desirable in the biomedical field due to their sensitivity to the physiological or biological environment where they are used [10]. They are also becoming increasingly important materials for pharmaceutical applications for the in situ delivery of active agents [11,12]. Moreover, hydrogels present 3D polymeric networks whose microstructure and porosity mimic the extracellular matrix and provide an environment in which cells can adhere, proliferate and differentiate [13,14].

Polyvinyl alcohol (PVA) hydrogels prepared using freeze/thaw techniques have great potential for biomedical applications such as its biodegradability [15–17] . Suzuki and Hirasa [18] presented some of the first work using cryogels with PVA [19]. Freeze/thawed gels are formed by freezing the polymeric solution. Upon freezing the solvent, crystals grow until they meet the facets of other crystals. The effect of these crystals is the formation of a porous system upon thawing [20–22].

pH-sensitive hydrogels containing polyacrylic acid (PAA) has been widely used in the area of drug-delivery systems principally due to its biocompatibility [23,24]. pH-sensitive polymers consist of pendant acidic or basic group that either accept or release protons in response to changes in environmental pH. Additionally, the incorporation of a co-polymer such as PAA that will contribute to hydrogen bonding can increase the strength of the hydrogel [19]. The application of PVA with PAA has been already reported and its potential applications due to their high swelling capability coupled with good mechanical properties [25,26]. However, the biggest drawbacks of these hydrogels in orthopaedic applications are their lack of bioactivity and their low resistance to the compression [27]. The latter is related to the swelling mechanism of hydrogels which swell due to electrostatic repulsions between the polymer chains [28]. This leads to a reduction in intermolecular bonding between the polymer chains and thus a mechanically weak structure. To overcome this issue, researchers have utilized hydrogels as a matrix in composites containing ceramics such as β-Tricalciumphosphate (β-TCP) which has been shown to enhance the physical bonding to the polymer chains [29–31]. Ceramic components also supply the bioactivity, osteoconductivity and

osteoinductivity to the composite. However, the field of ceramic hydrogels still needs further investigation since it is new and is still improving [32,33]

Hydroxyapatite (HAp) which is the mineral composition of bones, has been studied as a in these applications but it has poor *in vivo* solubility and slowly bioresorbs with traces of it remaining several months after implantation [34]. For this reason, tricalcium phosphate (TCP) is preferentially used as an alternative ceramic in this field [35,36]. Ceramic materials such as β-TCP are based on the chemical composition of hydroxyapatite [36,37]. β-TCP has a higher solubility compared to HAp and has improved osseointegration properties [38]. However, one of the biggest drawbacks of ceramics remains their low flexibility [39].

Therefore, in the current study polymeric/ceramic composites with different porosity distributions, which utilized PVA and PAA blends as the polymer matrix to provide elasticity, swelling capability and as a carrier vehicle for antibiotics, were combined with a ceramic material whose composition is based on β-TCP as majoritary phase, Wollastonite and $MgSiO_3$. TCP supplied Ca^{2+} and PO_4^{3-}, which are the main ions present in bones. Beta phase was choice as most soluble phase of TCP. Wollastonite was added in order to enhance the ceramics solubility and also supplying Si which stimulate osteoinduction [40]. In case of $MgSiO_3$, it was selected in order to supply Mg, which is present in bones and its absence results in bones with poorer mechanical properties [41]. Nanosilicates with Mg^{2+} contain as a hydrous sodium lithium silicate has been investigated in terms of the orthosilicic acid $Si(OH)_4$ capability to promote collagen type I synthesis and osteoblast differentiation via Wnt/β-catenin differentiation and their interaction with the gel [i]. It is well known that recent progresses in nanotechnology has stimulated the development of multifunctional biomaterials for tissue engineering applications [ii] [iii]and inorganic nanoparticles improve mechanical properties of hydrogel compared with microparticles. However, in this study ceramic composition was processed to obtain microporous ceramic grains. Microparticles and granulates have been suggested to simulate inorganic phase of bone extracellular matrix. Microporosity has been developed in these grains and granulates in order to helps and control solubility processes. Ceramic materials were dispersed in the polymer matrix which was solubilized with water and the final 3D construct was physically crosslinked using various freeze thawing (F/T) cycles. It is hypothesized that this combination of materials will have enhanced mechanical properties due to favorable intermolecular bonding compared to the hydrogel matrix alone and that it can be utilized for the in situ delivery of antimicrobial agents for the treatment of osteomyelitis. Furthermore, ceramic grains with different porous size distributions were developed with the aim to evaluate possible changes on physical properties of the final polymeric-ceramic composites as a result of differences in the impregnation process.

MATERIALS AND METHODS

Materials

PVA, PAA, ciprofloxacin and Phosphate Buffer Saline (PBS) were supplied by Aldrich, Ireland. Pans used for DSC were obtained from TA instruments, Ireland.

Ceramic fabrication

Ceramic grains are obtained from a initial composition of 60% tricalcium phosphate (TCP), from Carlo Erba, 25% Wollastonite (W), NYAD 1250 and 15% Talc, from Sigma Aldrich (wt%). Powders of raw materials were mixed by attrition milling for 1h, dried at 60°C and sieved through a 100µm pore size. Powders were compacted by uniaxial press at 1000 KPa/cm^2 and sintered at 1050°C for 2h. This temperature was selected as it is below the sintering temperature of this composition and results in materials with high porosity and crystalline phases characterized with higher solubility [42].

After thermal treatment β-TCP, Wollastonite 2M and MgSiO3 phases are obtained (%wt). Bulk samples obtained were ground and sieved with pore sizes of 45µm to 100µm to prepare grains with monomodal porosity distribution.

In order to fabricate grains with hierarchical porosity with bimodal distribution, grains previously obtained and prepared as described above, were compacted by uniaxial press at 1000KPa/cm^2 and sintered at 1050°C for 2h. Again, bulk samples obtained were ground and sieved, in this case, between 100 µm to 300 µm. These two different porosity size distributions were selected with the aim to assess the differences promoted in the finals 3D polymer composite in terms of the mechanical and swelling properties.

Polymeric-ceramic composition formulation and fabrication of composites

Physically cross-linked hydrogels were prepared by dissolving known concentrations of PVA, with average molecular weight of 195,000 and a percentage of hydrolysis of 98% (Mowiol 56-98) at 5% concentration (w/v) in distilled water (DH2O), at 80 °C with constant stirring until the complete solubilization of the PVA was achieved. This concentration was empirically determined to achieve low stiffness material [43] as it would also be able to detect any structural changes through-out the polymer. Subsequently, ceramic grains which were either monomodal (M) or Bimodal (B) were dispersed in the polymer solution at either 5 or 25 wt% of PVA, and finally PAA with molecular weight of 3,000,000 at concentration of 50% (w/w) of the weight of PVA was added in the mixture at ambient temperature.

Once a homogeneous solution was produced a diaphragm vacuum pump (LABOPORT®-SD, chemically-resistant) was used for remove the remaining bubbles visible in the solutions under a maximum vacuum of 10 mbar for 10 s. Finally, the samples were rapidly frozen to constant temperature of -80 °C for two hours in an ultra-low temperature freezer (Innova U535). The frozen solutions were then thawed in an oven at 25º C. This procedures performed either one (1X) or five (5X) times as outlined in Table 1. An oven (MINO/50) was used for 24 hours at 30 °C to remove the water from the hydrogels until the samples are completely dried. Samples used in antimicrobial activity tests were sterilized by placing them under UV curing system (Dr. Grobel UV-Electronik BmbH) with an average intensity of 10 mW/cm2.

TABLE 1. Summary of the Polymeric-ceramic samples prepared.

Sample Code	Grains with monomodal porosity (%wt)	Grains with bimodal porosity (%wt)	F-T cycles
PVA 1X			1
PVA 5X			5
PVA PAA 1X			1
PVA PAA 5X			5
M 5% 1X	5		1
M 5% 5X	5		5
M 25% 1X	25		1
M 25% 5X	25		5
B 5% 1X		5	1
B 5% 5X		5	5
B 25% 1X		25	1
B 25% 5X		25	5

Attenuated total reflectance Fourier transform infrared spectroscopy Fourier transform infrared (ATR-FTIR)

Attenuated total reflectance Fourier transform infrared spectroscopy (FTIR) was carried out using a Perkin Elmer Spectrum One spectrometer fitted with a universal ATR sampling accessory. All data was recorded in the spectral range of 4000–520 cm-1 utilsing a 4 scan per sample cycle. Subsequent analysis was carried out using Spectrum software.

Scanning electron microscopy (SEM)

Composite morphology was observed using a Mira SEM (TESCAN Perfomance in Nanospace) in back scattered electron (BSE) mode using magnifications which ranged from 50-500x. Prior to scanning the samples were sliced to obtain cross-sectional regions. The samples also were sputtered with a gold using Baltec SCD 005 for 110 s at 0.1 mBar vacuum before testing yielding a coating of ca 110 nm. Energy Dispersive X-ray (EDX) analysis was performed with an Oxford instruments detector was used to confirm the elements composition of the composite components.

Mercury Intrusion Porosimetry

Pore size distributions of ceramics grains materials were measured in a PoreMaster® from Quantchrome Instruments.

Differential Scanning Calorimeter

DSC analysis scans were obtained from using a DSC TA Q2000 from TA instruments. As hydrated gels did not comprise sufficient polymeric material to detect thermal transitions all samples were dried in an oven at 30ºC for 48 hours prior testing the samples. Sample weights between 9-12 mg were measured and encapsulated in sealed aluminum sample pans. The samples were tested using a temperature ramped from 0°C to 250°C at a rate of 10°C/min with an empty crimped pan used as a reference. The results were plotted as a function of heat flow (W/g) against Temperature (°C).

Rheological measurements

Rheology tests were carried out using an AR 1000 rheometer from TA instruments. Frequency and strain sweeps were carried out using the parallel plate method with Peltier plate temperature control. A 20 mm steel plate was used as the top geometry. A low frequency and low strain range was adopted. A frequency sweep was applied at a range of 0.1 – 100 Hz and a strain sweep was applied from 1.8E−4 to 1E−3 at a frequency of 1 Hz. In all cases a compression load of 2 ± 0.5 N was exerted on the swollen hydrogels during testing and data was presented as mean of two measures.

2.8 Swelling behaviour.

Swelling studies of the composite samples were carried out in PBS at pH 7.4. For the swelling properties, the PVA hydrogels was measured gravimetrically [44]. To measure the swelling kinetics, the pre-weighted samples were immersed in PBS. The excess surface solution was gently removed with paper and the swollen samples were weighted at various time intervals. The swelling ratio percentage of a hydrogel can be defined as:

$$S(\%) = \frac{(Ws - Wd)}{Wd} \times 100$$

$$S(\%) = \frac{Ws - Wd}{Wd} \times 100 \qquad (1)$$

where S(%) represents the weight of the swollen hydrogel at an specific time, also known as water uptake content, and Wd is the hydrogel dried mass before beginning the swelling studies.

Antibacterial evaluation.

To examine the antimicrobial activity, ciprofloxacin powder of 5wt% was added to the hydrogels and waited until total solubilization at room temperature prior the freeze/thawing. Resistant bacterial strains were inoculated into 10 ml of sterile nutrient broth, and incubated at 37 °C for 8 h. The bacteria Staphylococcus Aureus was used with approximately 108 colony forming units (CFU) of S. Aureus (ATCC 25923). Each culture was swabbed on the surface of sterile nutrient agar plate. In each agar plate, three wells were prepared with the help of sterilized cork borer of 10 mm diameter. In the wells of each plate, hydrogels samples were inserted and 50 µl of PBS (pH 7.4) was added to induce swelling. For each condition there were four plates. cultured on each agar plate. The plates were incubated for 24 h at 37° C. If inhibitory concentrations were reached, there would be no growth of the microbes, which

could be seen as a clear zone around the disc specimens.

Statistical analysis

Each experiment was performed in duplicate and analyzed using ACTION software. Results are expressed as mean ± standard deviation. One way analysis of variance (ANOVA) was carried out followed by Tukey`s post hoc test for comparisons between all groups. The level of significance was set at $p \leq 0.05$.

RESULTS

Ceramics morphology

Figure 1 shows SEM micrographs of ceramic grains used in the composites: with grain sizes between 45 to 100 µm (Fig. 1a ad b) and grain sizes between 100 to 300 µm (Fig. 1d and e). In both cases, as a result of some grains collapse, it can be observed the presence of numerous smaller grains. Have to be noted the low temperatures applied during the compacting thermal treatment in order to obtain high porosity. Ceramic grains from Fig 1 (a), were obtained by just one thermal treatment of the raw materials previously mixture and compacted as was described in *2.2 Ceramic fabrication*. In this micrograph it can be observed grains sizes between 45 to 100 µm. Images of these grains at higher magnifications (Fig 1b) show that they are composed by two different smaller grains; rounded grains, corresponding to calcium phosphate phase, and fiber grains, corresponding to calcium silicate phase. Moreover, the micrograph shows an interconnected porosity with monomodal pore sizes, in agreement with the distribution obtained by Hg porosimetry (Fig 1c, black line). It shows the pore size distribution between 0,1 to 4 µm composed at least by two populations, one at 0,3 µm due to the pore diameter and other one at 0,6 µm as result of smaller collapsed grains compression during the measurement.

Fig. 1(d and e) shows grains obtained after the compaction and a second thermal treatment realized over the previous ones, grains with monomodal pore size distribution. Sizes of these grains are between 100 to 300 µm. They are composed by grains described in Fig. 1(a and b), which are embed in a matrix of smaller grains. These grains possess an interconnected porosity with more complex signal of pore size distribution. Pore sizes, also measured by Hg porosimetry (Fig 1c, green line), shows a profile between 0,1 to 5 µm composed at least by three signals. At 0,3 is found a signal matching with the porosity corresponding to grains between 45 to 100 µm. Between 0,4 to 4 µm the profile is complex and probably due to at least two signals, the corresponding to the compression of smaller collapsed grains at 0,6 µm and the corresponding to wider pores obtained during second compaction and thermal treatment.

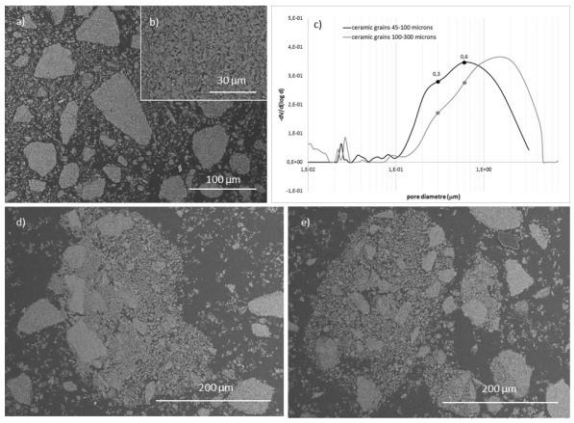

FIGURE 1 SEM micrographs from ceramics grains section a) grains with monomodal pore size distribution b) magnification of grains with monomodal pore size distribution c) Hg intrusion porosimetry of monomodal grains (grain sizes between 45 to 100 microns, black line) and bimodal ceramic grains (grain sizes between 100 to 300 microns, green line) and d) and e) grains with bimodal pore size distribution.

In both cases the low sintering temperatures used give rise to a low densification, which is

interesting for the aim to obtain high porous grains. Also can be observed some ceramic grains have not been enough densified and are disaggregated.

Fourier transform infrared (FTIR)

FTIR was used to determine if intramolecular bonding occurred between the ceramic ad polymeric phases of the composite. The FTIR spectra of reference hydrogels, pure ceramics and polymeric-ceramic composites are shown in Figure 2. The ceramics had characteristic peaks in the range between 800 and 1200 cm^{-1}. In the current study, signals at 682 and 902 cm^{-1} can be assigned to SiO_2 groups of Wollastonite [42]. Signals at 938, 968, 1022 and 1107 cm^{-1} are attributed to $(PO_4)^{3-}$ groups from TCP [31,43]. The successful incorporation of the ceramic into the composite structure is evidenced by these correspondent peaks in the composite structure. However, the position of these peaks has sometimes shifted as a result of intramolecular bonding with the hydrogel matrix. An example of this can be seen in Figure 2 where the peak corresponding to TCP at 969 cm^{-1} appears at 946 cm^{-1} for composite sample M-5%-5X. When different ceramic porosities are considered it appeared that these correspondent peaks became more defined for composites which incorporated bimodal ceramic granules compared to monomodal granules. In figure 2 this is evidenced by the formation of a clear TCP peak at 1022 cm^{-1} for bimodal composites whereas this appears as a shoulder in monomodal composites.

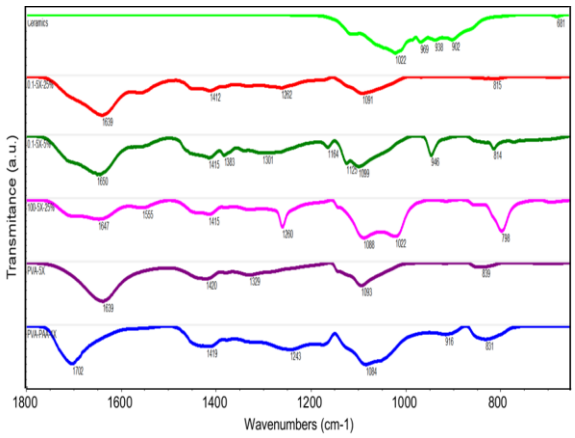

FIGURE 2. FTIR spectra of the ceramic, matrix and various composites studied.

In terms of the hydrogel matrix, the polyvinyl alcohol and polyacrylic acid peaks are generally correspondent to alcohol and carboxylic acid groups. The large band between 3500 and 3200 cm^{-1} are due to the stretching O-H [44,45]. The asymmetrical and symmetrical stretching of C-H are found at 2840-3000 cm^{-1}. With addition of PAA some of the peaks becomes more defined and new bands were observed corresponding solely to PAA between 1750-1710 cm^{-1} which are characteristic bands of C=O and C-O stretching of carboxylic groups [46,47]. The intensity of the peak at 1702 cm^{-1} which corresponds to the dimeric form of carboxylic groups (Devine & Higginbotham, 2003) shows a reduction in peak intensity with the addition of ceramics which indicates the formation of new intermolecular interaction between the ceramic and the PAA phase of the matrix material at the expense of the cyclic dimer interactions of PAA. This correlates to the formation of a new peak in the spectrum containing ceramics in the region of 1640 which is characteristic of carbonyl C=O groups which are ionically bonded (typically hydrogen bonded) [48] in this instance to the ceramic material. Additionally, a peak forms in the composite between 1555 and 1560 cm^{-1} which corresponds to ionic bonding of the carbonyl C=O group of PAA.

In the spectra of composites containing bimodal ceramics, the intensity of the peaks appears to increase. For example in sample B-5x-25% there is a peak at 1272 cm^{-1} that corresponds to -CH_2- vibrations of carboxylic acid groups of PAA which becomes more intense due to the ceramics particle [48,49]. The peak at 1140 cm^{-1} corresponds to crystalline PVA. It is very weak in some of the composites indicating that the ceramic may have interfered with the crystallization process during F/T. However, the C=O peak due to stretching in the crystalline region of PVA is further increased with ceramic samples with 5 F/T cycles. Finally, a peak at 798 cm^{-1} is characteristic of CH_2 twisting and stretching in the PAA moiety.

Hydrogels morphology

SEM analysis was used to visualize the ceramic dispersion in the matrix and the overall morphology of the composite. The composite morphologies can be observed in figures 3-4, which represents the polymers with different Freeze/Thaw cycles, porosities and concentrations. Images of the surfaces and cross-section of these composites are presented.

It can be seen that the ceramics particles were dispersed throughout the polymer structure. However, it is possible to identify groups of aggregates of ceramics particles on samples containing 5% and 25% ceramics. With higher concentrations of ceramics more aggregate groups were observed as expected. Furthermore, with an increase of ceramics concentration it improves the network formation and affects its internal porous structure. With different porosities it can be noted that different internal porous shapes were obtained, hydrogels with monomodal ceramics gave rise to bigger and more open pores than the hydrogels with the bimodal porosity. On the other hand, hydrogels with bimodal ceramics gave rises to thicker and robust network walls.

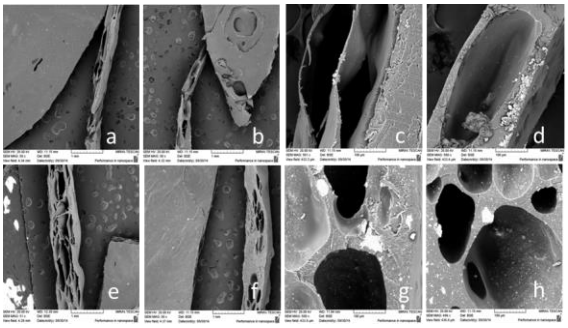

FIGURE 3. SEM images of the hydrogels: M 5% 1X (a) 50x and (c) 500x; B 5% 1X (b) 50x and (d) 500x. M 5% 5X (e) 50x and (g) 500x; B 5% 1X (f) 50x and (h) 500x.

Increasing the number of Freeze/Thaw cycles tended to result in a related increase in porosity of the hydrogel. Moreover, samples with five Freeze/Thaw cycles showed a more defined networks with higher number of interconnected pores.

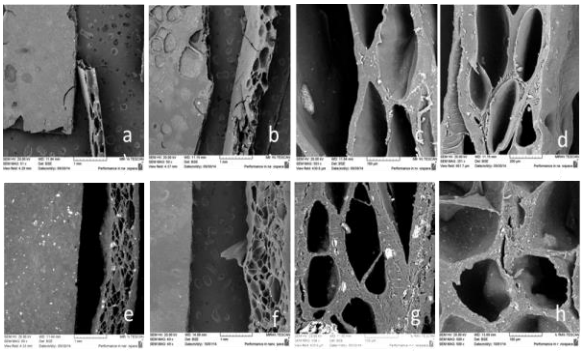

FIGURE 4. SEM images of the hydrogels: M 25% 1X (a) 50x and (c) 500x; B 25% 1X (b) 50x and (d) 500x. M 5% 25X (e) 50x and (g) 500x; B 25% 1X (f) 50x and (h) 500x.

Swelling study

The swelling study was based on the ability of the composite to allow the migration of water from surrounding areas into the pre-existing spaces in the hydrogel chains. It promotes the physiological stability of scaffolds, permeability of the biomolecules and low interfacial tension [50]. The values obtained are shown in Fig. 5 which displays the swelling behavior of the studied composites. The addition of ceramics to the hydrogel matrix resulted in an increase in

the percentage swelling of the composites in comparison to PVA (350%) and PVA+PAA (830%). Composites with one F-T cycle exhibited a very rapid swelling rate in contrast with the ones with five F-T cycles and reached equilibrium after three hours. Conversely, hydrogels obtained after five F-T cycles absorbed water slower and did not reach equilibrium until 30h in PBS. When the ceramic porosity was assessed, in general there is little difference in the total swelling of monomodal and bimodal ceramics with the exception of 5% ceramic following 5 F-T cycles where it was found that the monomodal containing composites swelled considerably more than the corresponding bimodal containing composite.

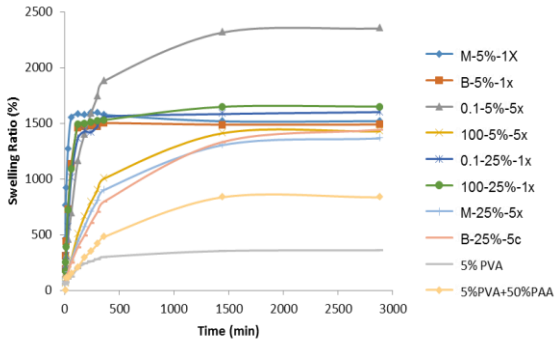

FIGURE 5. swelling behavior of the studied hydrogels in buffer solution pH 7.4.

Differential scanning calorimetry (DSC)

DSC measurements were performed to determine the thermal characteristics of the composites. The thermograms for the individual components are listed on Fig. 6. The DSC thermograms obtained from the different polymer-ceramic composites developed by different Freeze/Thaw cycles can be seen on Fig. 7 and 8.

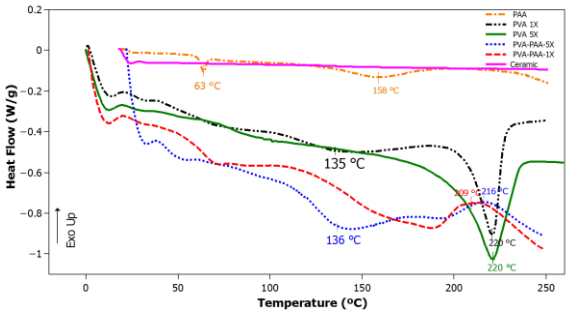

FIGURE 6. DSC thermograms of the base materials utilized in the manufacture of Freeze/Thawed composites.

Starting from PVA which had undergone one Freeze/Thaw cycle, it is possible to identify a relaxation in the region of 100-200 ºC (T_g= 135 °C), known as β_c relaxation which is due to relaxation of the domains in the crystalline regions of the PVA. The crystalline melting temperature was found in the region of 200-250 ºC (T_m= 220°C), was caused by the melting of the crystalline domains of PVA [51]. With an increase on the number of Freeze/Thaw cycles, the melting point peak size increases and broadening of the peak, indicating an increase in crystallinity [52].

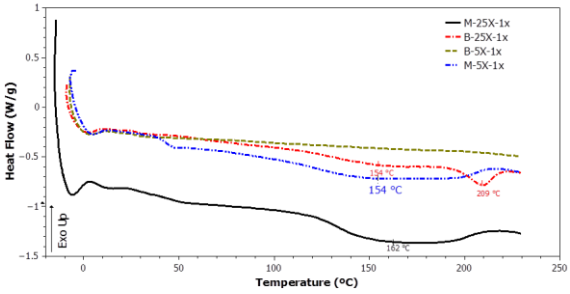

FIGURE 7. DSC from 5%PVA and 50%PAA 5 and 25% of ceramic grains with monomodal and bimodal porosity and 1 cycle F-T.

The thermogram of pure PAA in powder form shows that the α relaxation peak of the PAA is represented by the step change at 63 °C. The melting point of the pure PAA is at 157 °C which corresponds to other values reported in literature [46]. With the addition of PVA, the blend of PVA+PAA shows a relatively broad exothermic glass transition (one F/T; T_g = 209°C,

five F/T; T_g= 216°C). The Tm appeared to have increased to over 250°C. The heat flow profile for the ceramic is also included (Fig. 6) indicate no melting point in the region studied.

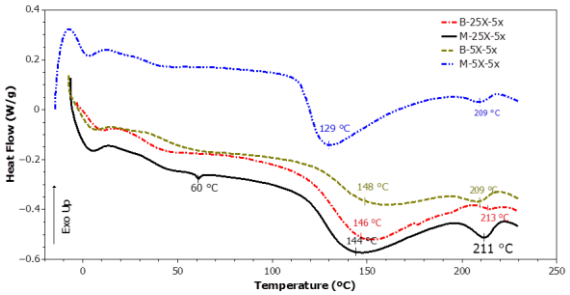

FIGURE 8. DSC from 5%PVA and 50%PAA 5 and 25% of ceramic grains with monomodal and bimodal porosity and 5 cycles F-T.

With the addition of the ceramics, composites following one Freeze/Thaw cycle (Fig. 7) had their relaxation curves and melting points reduced in comparison to the samples without ceramics. With higher concentrations of the ceramic, the samples starts to have more defined signals and the same profile as without ceramics can be observed in these samples. However, for the sample with bimodal porosity and at higher concentration of ceramics there was an endothermic melting peak associated with PVA. The samples with five Freeze/Thaw cycles also exhibited an endothermic transition melting peaks for PVA on all of the samples. The sample with monomodal porosity and 25% of concentration shows the 'α' relaxation peak of the PAA at °60 C, which approximated that of pure PAA.

Rheological measurements

Rheology measurements were recorded to investigate any relative differences in strength with the addition of ceramics on these hydrogels. The log plots for the hydrogels systems are shown in Fig. 9.

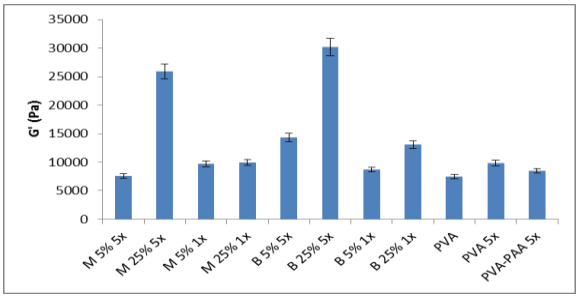

FIGURE 9. Strain sweep step from composite samples with ceramic grains with monomodal and bimodal porosity at 5% and 25% in ceramic content and 1 and 5 F-T cycles.

The elastic and viscous properties of a fluid are represented by two critical viscoelastic parameters, namely storage (G') and loss (G'') modulus, respectively. The frequency sweep tests shows that both the storage modulus G' and the loss modulus G'' are not dependent of the frequency variation between 0.1 and 100 Hz. Best result was obtained for samples M 25% 5X and B 25% 5X which are the ones with higher percentage of ceramics and higher FT cycles number as happen in compression test.

The average value of G' for each type of composite was calculated and results are shown in Fig. 10. Hydrogels are known as viscoelastic materials, however, rheological results indicate that with the addition of TCP caused an increase in the strength of the swollen composite as indicated by an increase in the G'.

Additionally, increasing the number of Freeze/Thaw cycles also caused a general increase in the mechanical properties of the composite. However, when adding PAA a noticeable decrease in storage modulus occurs, which is also confirmed by other groups [25,48]. The composites with the highest mechanical properties in the swollen state were samples B 25% 5X and M 25% 5X.

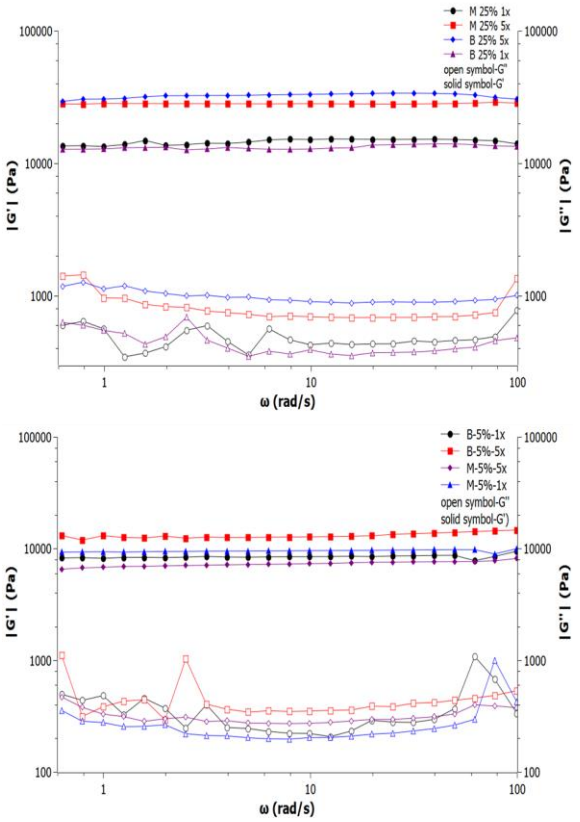

FIGURE 10. Strain sweep step from composite samples with 5% and 25% of ceramic grains with monomodal porosity.

Antimicrobial activity tests

The antimicrobial activities of ciprofloxacin incorporated into the structure of the prepared composites were investigated.

TABLE 2. Inhibition pattern of all samples against S. aureus (ATCC 25923). *p ≤ 0.05, sig. = 1 for 4 plates (n=12). There is a significant difference between the levels indicated by arrows.

	M-25%-5x	*	B-25%-5x
Mean(mm)	35.7*		32.4*
SD(mm)	0.9		0.7
Min(mm)	34.6		31.6
Max(mm)	36.9		33.5

Inhibition zone formation confirms that these samples had antimicrobial activity with the addition of ciprofloxacin against Staphylococcus aureus ATCC 25923 (Table 2). Composites which contain ceramics with Monomodal porosity are statistically more effective than the bimodal porosity.

DISCUSSION

To meet the requirements of an ideal bone substitute material, a material should process an array of properties which are not easily fulfilled using a single material. Hence, combinations of materials as is the case for natural bone which contains minerals, collagen, water, proteins, lipids, vascular elements and cells [53] may prove to be the most effective way of meeting these requirements. In the current study the polymer phase utilized is a PVA-PAA blend as physically crosslinked structures can be produced from this blend [25] and as it is of a synthetic nature, there is low batch to batch variability. The ceramic component composition was based on β-TCP, Wollastonite and Talc. β-TCP was selected because of its higher solubility compared with other TCP phases. It supplies Ca^{2+} and PO_4^{3-} which are the main elements of mineral phase in bones. Wollastonite was selected due to its good solubility and it also supplies Si which stimulates osteoinduction [40]. Talc was selected to supply Mg which is found in the mineral phase of bones and its absence results in a reduction in mechanical properties [41]. These components were mixed, compacted and sintered together to create porous structures. Porosity parameter has been already studied with different aims. For example, the effect in the improvement of mechanical properties when poly (Ɛ-caprolactone) was used to infiltrate calcium phosphate scaffolds with monomodal and bimodal porosity has been studied [54]. A low sintering temperature was selected as it was sufficient to sinter the components together but did not cause effect the porosity of the ceramic and prevented TCP from phase changing from beta to alpha phase as beta phase TCP is more desirable in terms of

solubility. The polymer and ceramic materials were mixed and physically crosslinked using a number of freeze thaw cycles to determine if this was a feasible fabrication method for producing drug loaded composite structures. This method of crosslinking was selected as it can be achieved without the use of crosslinking agents and initiators which could potentially increase the toxicity of the composite. Furthermore, in natural bone repair, fractures heal in a six to eight week time period [55]. If the scaffold is chemically crosslinked the scaffold will not dissolve and hence degradation of the polymers is based on enzymatic or hydrolytic pathways [5]. This can take in excess of 8 weeks especially in systems containing ceramics which enhance the intramolecular bonding between the molecular chains as this could limit fluid infiltration. The method of producing composite structures utilizing a F/T cycle method also enables the incorporation of active ingredients into the composition of the composite and as no chemical reaction occurs, there is little or no risk of affecting the functionality of efficacy of the active ingredient. During the fabrication process all individual components were dispersed without difficulty.

The difference in the structural changes based as observed using FTIR can be induced by the size of the ceramics particles, which can influence the adhesion in the hydrogels [56] which then leads to reinforcement of intermolecular and intramolecular bonds. It was noted that hydrogels with higher ceramic content had more bands than the ones with lower concentrations. With more ceramics in the hydrogels, more bonds can be formed which reinforces the structure of the composite. Analysis of the FTIR spectrum of the hydrogel matrix in this work indicated that the incorporation of PAA enhanced intermolecular bonding through the formation of cyclic carboxylic acid dimers which corresponds to the formation of a peak in the region of 1700 cm^{-1} [57]. With the incorporation of the ceramic component this intermolecular bonding appears to have reduced in preference to the formation of intramolecular bonds between the ceramic material and the carboxylic group of PAA as evidenced by the formation of a peaks in the region of 1640 to 1650 cm^{-1} and 1550 to 1560cm^{-1} both of which are indicative of hydrogen bonding of the carboxylic group of PAA. Furthermore, this increase in intramolecular bonding appeared to interfere with the crystallization of the PVA phase of the composite as evidenced by the reduction in the peak at 1411 cm^{-1} which corresponds to crystalline PVA. Similar findings were observed by [58] who found that the incorporation of calcium into an alginate system resulted in an 'egg-box' type structure, where the intermolecular bonding of the polymer was reduced in preference to intramolecular bonding with calcium.

When the resultant composites were examined under SEM in their dehydrated form, it was found that the porosity of the scaffold was dependent on both the number of F-T cycles and also on the level of ceramic component in the composite. Increases in the number of freeze thaw cycles produced a porous structure that appeared to exhibit an increase in wall thickness and had a structure similar in appearance to the structure of cancellous bone. Higher values of ceramic in the composite appeared to produce a higher level of interconnectivity in the porous structure. When monomodal and bimodal ceramics were compared it was found that composites containing monomodal ceramics appeared to have a large thin walled pores, especially after one freeze thaw cycle compared to an increase in wall thickness for composites containing bimodal ceramics. This may be due to the porous structure of the bimodal grains which allowed better polymer infiltration and therefore better bonding to the ceramic grains. This effect was less evident following five F-T cycles, as the increased number of F-T cycles compacted the molecular chains potentially disguising this effect.

Swelling analysis of the composites indicated that the composites swelled more than the matrix alone. [28] reported a similar phenomenon due to the incorporation of Ca^{2+} and Mg^{2+} ions which were shown to increase swelling. However, composites which underwent five F-T cycles swelled at a slower rate than samples which underwent one F-T cycle. This was due to the lower level of physical crosslinking achieved using 1 compared to 5 F-T cycle, and is closely related to the morphology of the composites where we have shown that an increase in F-T cycles results in an apparent enhancement in the wall thickness of pores in the composite. In these samples, the watery media needed increased time to penetrate the inside of the sample and fill the pores. However, after one F-T cycle the thin wall structure and relatively larger pores enabled water to diffuse quickly into the composite and fill the pores more rapidly. Furthermore, electrostatic repulsion and crosslink disruption favor the increase in swelling ratio observed for hydrogels [28]. Nevertheless, with five F-T cycles the reduction in swelling indicates that this electrostatic repulsion has been overcome with intramolecular bonding.

Thermal analysis of the composite structures indicated that the beta transition temperatures obtained for PVA had increased in comparison to PVA alone but had reduced in comparison to the PVA-PAA blend used as the matrix material. These results indicate a stiffening of the polymer with the incorporation of PAA, likely due to intermolecular bonding of the PAA moiety of the matrix as evidenced by FTIR which showed the formation of a PAA dimeric group. However, the incorporation of the ceramic component acted as a plasticizer by inhibiting a degree of intermolecular bonding in the polymer matrix which resulted in a decrease in the beta transition value. The T_m of PVA is in the region of 210 °C. With the incorporation of PAA this increases to a value in excess of 250 °C indicating a reduction in crystallinity which concurs with FTIR findings. However, the incorporation of the ceramic component into the composite reduced the melt temperature back to that of PVA. This was especially evident after 5 F-T cycles. These samples have a higher degree of hydrogen bonding than composites with one F/T cycle due to tightening of the molecular chains caused by the F-T process. On the contrary, the samples containing bimodal ceramic grains at 5% of concentration showed no melting point peak within the temperatures tested which is similar to the thermogram of the PVA-PAA matrix alone. This indicates that the level of ceramic was insufficient to disrupt PAA intermolecular bonding to a high degree.

Rheological measurements were used to compare the relative strength of different composites. The mechanical properties of bone tissue engineering constructs is often overlooked but it is an essential requirement for the success of a treatment as the inability of scaffolds to contribute to load bearing and hence cell signaling can itself lead to complications such as non-unions [59]. Using rheological analysis the storage modulus of the composites was recorded. The storage modulus is a measure of the recoverable energy in a system and the materials ability to recover following strain. Hence, this property is dependent on the level of crosslinking in a system. Therefore, in the current study any factors which increased the physical crosslinking in the system would cause an increase in storage modulus. Based on the current findings it can be said that both an increase in the concentration of TCP and an increase in the number of F/T cycles increased the physical crosslinks in the system as was indicated by FTIR analysis and thermal analysis measurements. Frequency-sweep analysis indicates that the composites behave like a solid as indicated by the linear storage modulus response which was higher than the corresponding loss modulus. This is a characteristic feature of crosslinked hydrogel [60]. In this work the maximum storage modulus recorded was approximately 30KPa. These results correspond favorably with the results from other studies where composite materials

were assessed for bone regeneration applications and their storage modulus values were reported to be between 300 Pa to 15KPa [31]. Nevertheless, this system is weaker than similar systems prepared by chemically crosslinking where values of 60-80KPa have been reported [31]. However, Killion et al. [31] reported data based on a highly chemically crosslinked composite which would not readily degrade to facilitate bone formation. In relation to the porosity of the ceramic components, the porosity was not found to contribute greatly to the final mechanical strength of the composite. Nevertheless, increasing the number of F-T cycles greatly improved the crosslinks density and intramolecular bonding of the composites which resulted in the general increase in mechanical properties corresponding to the increase in F-T cycles.

Furthermore, a biocompatible material is preferable for the delivery of active pharmaceuticals as 100% drug release can be ensured. It is known that ciprofloxacin is a good antibiotic against *S. aureus* due to osteomyelitis [61]. In the current study, it was found that not only could ciprofloxacin be easily incorporated into the composite structure during fabrication, but the F-T process was also found not to effect the antimicrobial activity of ciprofloxacin. This was evidenced by the control of S. aureus surrounding the scaffold when ciprofloxacin was incorporated into the system.

CONCLUSION

In this work we have evaluated the potential for novel PVA/PAA/TCP composites fabricated using the F-T process for use as a bone healing applications. The results of the study indicate that properties of the composite were dependent on the intermolecular and intramolecular bonding between the different components in the composite and this could be controlled by varying the concentration and composition of the different components. Additionally, increasing the number of F-T cycles further improved the intermolecular and intramolecular bonding which enhanced the properties of the final composite. Finally, the composite was used as a carrier for a clinically relevant antimicrobial agent. Results of zone of inhibition indicated that the efficacy of the antimicrobial agent was not affected by the incorporation method and as such the composite developed in the current study has potential in orthopedic applications where the patient is in a high risk group for getting osteomyelitis.

ACKNOWLEDGEMENTS

This work was supported by the NEW GEN (MP1301) Biomimetic and Customized Implants for Bone Engineering COST Action Short Term Scientific Mission, a Marie Curie International Outgoing Fellowship within the 7th European Community Framework Programme (Project 298107; NanoFact), Biomateriales cerámicos multifuncionales con estructuras jerarquizadas para regeneración ósea y/o liberación controlada de agentes bioactivos, Plan Nacional 2013 Proy I+D+i "Retos Investigación" Prog. Retos de la Sociedad, MAT2013-48426-C2-1-R, and by research grants from science without borders and Capes.

REFERENCES AND NOTES

1 C. H. Evans, *Mayo Clin. Proc.*, 2013, **88**, 1323–1329.

2 G. M. Calori, E. Mazza, M. Colombo and C. Ripamonti, *Injury*, 2011, **42**, S56–S63.

3 R. Cancedda, P. Giannoni and M. Mastrogiacomo, *Biomaterials*, 2007, **28**, 4240–50.

4 Z. S. Patel, S. Young, Y. Tabata, J. a. Jansen, M. E. K. Wong and A. G. Mikos, *Bone*, 2008, **43**, 931–940.

5 A. Oryan, S. Alidadi, A. Moshiri and N. Maffulli, *J. Orthop. Surg. Res.*, 2014, **9**, 18.

6 J. Hatzenbuehler and T. J. Pulling, *Am Fam Physician. 2011 Nov 1;84(9)*, 2011, 1027–1033.

7 M. P. Staiger, A. M. Pietak, J. Huadmai and G. Dias, *Biomaterials*, 2006, **27**, 1728–1734.

8 V. Karageorgiou and D. Kaplan, *Biomaterials*, 2005, **26**, 5474–91.

9 D. Puppi, F. Chiellini, A. M. Piras and E. Chiellini, *Prog. Polym. Sci.*, 2010, **35**, 403–440.

10 N. A. Peppas, Y. Huang, M. Torres-Lugo, J. H. Ward and J. Zhang, *Annu. Rev. Biomed. Eng.*, 2000, **2**, 9–29.

11 D. M. Devine, L. M. Geever and C. L. Higginbotham, *J. Mater. Sci.*, 2005, **40**, 3429–3436.

12 J. A. Killion, L. M. Geever, D. M. Devine, H. Farrell and C. L. Higginbotham, *Int. J. Polym. Mater. Polym. Biomater.*, 2014, **63**, 641–650.

13 N. Rahimi, D. G. Molin, T. J. Cleij, M. A. van Zandvoort and M. J. Post, *Biomacromolecules*, 2012, **13**, 1448–1457.

14 H. Cui, Y. Liu, Y. Cheng, Z. Zhang, P. Zhang, X. Chen and Y. Wei, *Biomacromolecules*, 2014, **15**, 1115–1123.

15 O. Lopez, G. L. Sierra and G. Mejía, *Polym. Eng. Sci.*, 1999, **39**, 1346–1352.

16 S. Matsumura, N. Tomizawa, A. Toki, K. Nishikawa and K. Toshima, *Macromolecules*, 1999, **32**, 7753–7761.

17 T. Suzuki, in *J Appl Polym Sci Appl Polym Symposium*, 1979, vol. 35, pp. 431–437.

18 M. Suzuki and O. Hirasa, in *Responsive Gels: Volume Transitions II SE - 10*, ed. K. Dušek, Springer Berlin Heidelberg, 1993, vol. 110, pp. 241–261.

19 C. M. Hassan and N. A. Peppas, in *Advances in Polymer Science*, 2000, vol. 153, pp. 38–65.

20 A. Kumar, A. Srivastava, I. Y. Galaev and B. Mattiasson, *Prog. Polym. Sci.*, 2007, **32**, 1205–1237.

21 W. Wan, A. D. Bannerman, L. Yang and H. Mak, in *Polymeric Cryogels SE - 8*, ed. O. Okay, Springer International Publishing, 2014, vol. 263, pp. 283–321.

22 L. E. Millon, M.-P. Nieh, J. L. Hutter and W. Wan, *Macromolecules*, 2007, **40**, 3655–3662.

23 C. A. Schoener, H. N. Hutson and N. A. Peppas, *Polym. Int.*, 2012, **61**, 874–879.

24 E. S. Yim, B. Zhao, D. Myung, L. C. Kourtis, C. W. Frank, D. Carter, R. L. Smith and S. B. Goodman, *J. Biomed. Mater. Res. Part A*, 2009, **91**, 894–902.

25 M. J. McGann, C. L. Higginbotham, L. M. Geever and M. J. D. Nugent, *Int. J. Pharm.*, 2009, **372**, 154–61.

26 G. de Lima, D. Devine, C. de Alencar, A. Junqueira, R. Emanuel and M. Nugent, *Proc. 1st Int. Electron. Conf. Mater.*, 2014, **Vol. 1**, d006.

27 J. Zhu, *Biomaterials*, 2010, **31**, 4639–4656.

28 V. B. Bueno, R. Bentini, L. H. Catalani and D. F. S. Petri, *Carbohydr. Polym.*, 2013, **92**, 1091–1099.

29 Y. Dai, H. Liu, B. Liu, Z. Wang, Y. Li and G. Zhou, *Ceram. Int.*, 2015, 1–9.

30 W. Togami, A. Sei, T. Okada, T. Taniwaki, T. Fujimoto, S. Tahata, K. Nagamura, Y. Nakanishi and H. Mizuta, *J. Biomed. Mater. Res. Part B Appl. Biomater.*, 2015, **103**, 188–194.

31 J. A. Killion, S. Kehoe, L. M. Geever, D. M. Devine, E. Sheehan, D. Boyd and C. L. Higginbotham, *Mater. Sci. Eng. C. Mater. Biol. Appl.*, 2013, **33**, 4203–12.

32 S. Van Vlierberghe, P. Dubruel and E. Schacht, *Biomacromolecules*, 2011, **12**, 1387–1408.

33 W. Li, M. Pastrama, Y. Ding, K. Zheng, C. Hellmich and A. R. Boccaccini, *J. Mech. Behav. Biomed. Mater.*, 2014, **40**, 85–94.

34 P. D. Costantino, C. D. Friedman, K. Jones, L. C. Chow, H. J. Pelzer and G. A. Sisson, *Arch. Otolaryngol. Neck Surg.*, 1991, **117**, 379–384.

35 M. Jarcho, *Clin. Orthop. Relat. Res.*, 1981, **157**, 259–278.

36 M. Kamitakahara, C. Ohtsuki and T. Miyazaki, *J. Biomater. Appl.*, 2008, **23**, 197–212.

37 A. Kolk, J. Handschel, W. Drescher, D. Rothamel, F. Kloss, M. Blessmann, M. Heiland, K. D. Wolff and R. Smeets, *J. Cranio-Maxillofacial Surg.*, 2012, **40**, 706–718.

38 A. Ogose, T. Hotta, H. Kawashima, N. Kondo, W. Gu, T. Kamura and N. Endo, *J. Biomed. Mater. Res. - Part B Appl. Biomater.*, 2005, **72**, 94–101.

39 D. Chicot, *New J. Glas. Ceram.*, 2013, **03**, 16–28.

40 A. E. Porter, N. Patel, J. N. Skepper, S. M. Best and W. Bonfield, *Biomaterials*, 2004, **25**, 3303–3314.

41 A. Creedon, A. Flynn and K. Cashman, *Br. J. Nutr.*, 1999, **82**, 63–71.

42 T. Vázquez-Moreno and M. T. Blanco-Varela, *Mater. Construcción*, 1981, **31**, 31–48.

43 L. Berzina-Cimdina and N. Borodajenko, *Research of calcium phosphates using Fourier transform infrared spectroscopy*, INTECH Open Access Publisher, 2012.

44 G. I. Andrade, E. F. Barbosa-Stancioli, a. a P. Mansur, W. L. Vasconcelos and H. S. Mansur, *J. Mater. Sci.*, 2008, **43**, 450–463.

45 H. S. Mansur, C. M. Sadahira, A. N. Souza and A. A. P. Mansur, *Mater. Sci. Eng. C*, 2008, **28**, 539–548.

46 J. J. Maurer, D. J. Eustace and C. T. Ratcliffe, *Macromolecules*, 1987, **20**, 196–202.

47 S. Nesrinne and A. Djamel, *Arab. J. Chem.*, 2013.

48 J. Jose, F. Shehzad and M. A. Al-harthi, 2014.

49 J. Dong, Y. Ozaki and K. Nakashima, *Macromolecules*, 1997, **30**, 1111–1117.

50 F. Ganji, S. Vasheghani-Farahani and E. Vasheghani-Farahani, *Iran. Polym. J.*, 2010, **19**, 375–398.

51 J.-S. Park, J.-W. Park and E. Ruckenstein, *Polymer (Guildf).*, 2001, **42**, 4271–4280.

52 C. M. Hassan and N. a. Peppas, *Macromolecules*, 2000, **33**, 2472–2479.

53 R. Murugan and S. Ramakrishna, 2005, **65**, 2385–2406.

54 M. Peroglio, L. Gremillard, C. Gauthier, L. Chazeau, S. Verrier, M. Alini and J. Chevalier, *Acta Biomater.*, 2010, **6**, 4369–4379.

55 B. McKibbin, *J. Bone Jt. Surgery, Br. Vol.* , 1978, **60-B** , 150–162.

56 H. Priya James, R. John, A. Alex and K. R. Anoop, *Acta Pharm. Sin. B*, 2014.

57 D. M. Devine and C. L. Higginbotham, *Polymer (Guildf).*, 2003, **44**, 7851–7860.

58 A. S. Marriott, E. Bergström, A. J. Hunt, J. Thomas-Oates and J. H. Clark, *RSC Adv.*, 2014, **4**, 222–228.

59 W. J. King and P. H. Krebsbach, *Adv. Drug Deliv. Rev.*, 2012, **64**, 1239–1256.

60 D. Calvet, J. Y. Wong and S. Giasson, *Macromolecules*, 2004, **37**, 7762–7771.

61 J. K. Koort, T. J. Mäkinen, E. Suokas, M. Veiranto, J. Jalava, J. Knuuti, P. Törmälä and H. T. Aro, *Antimicrob. Agents Chemother.*, 2005, **49**, 1502–1508.

GRAPHICAL ABSTRACT

Maria Canillas, Gabriel Goetten de Lima, Miguel A. Rodríguez, Michael J.D. Nugent, Declan M. Devine

Novel bioactive composites fabricated by freezing-thawing method for bone regeneration applications.

A composite cryogel that produces high strength composites materials which can control the release of antimicrobial agents is the aim of this work. The constructs presents stronger values than similar materials in the literature and contain porous structure which is beneficial for vascular invasion and bone ingrowth. Since the fabrication method does not require any toxic elements, presents good biocompatibility and ability to control swelling, this system have great potential in the field of orthopaedics.

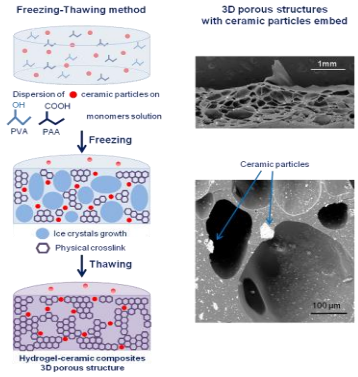

[i] Janet R. Xavier, Teena Thakur, Prachi Desai, Manish K. Jaiswal, Nick Sears, Elizabeh Cosgriff-Hernandezz, Ronal Kaunas and Akhilesh K. Gaharvar. Acsnano, 2015, Vol. 9, No 3, 3109-3118.

[ii] Nanomaterials for stem cells responses Punyavee Kerativitayanan, James K. Carrow and Akhilesh K. Gaharwar. Adv. Healthcare Mater. 2015, 4, 1600–1627

[iii] Novel Nanostructured Zn-substituted Monetite Based Biomaterial for Bone Regeneration. Sussette Padilla, Arcadio García de Castro, Ana Garzón-Gutiérrez, Lorena Benito, Silvia Enciso, Maria Canillas and Raúl G Carrodeguas. J Nanomed Nanotechnol 2015, 6:5. Doi http://dx.doi.org/10.4172/2157-7439.1000325